Methods for multiphase flows with high density ratio

By O. Desjardins† and V. Moureau‡

Two-phase flows with high density ratio and high shear are known to be challenging to simulate. In this work, two strategies for improving the robustness of high density ratio two-phase flow simulations are investigated. The first method, based on Rudman's work with the volume of fluid method (Rudman 1998), aims at improving the consistency between interface and momentum transport by using the interface position to estimate the density that appears in the momentum convection fluxes. The second approach effectively decouples gas and liquid velocities by introducing two distinct vector fields coupled through the pressure Poisson equation, in the spirit of the ghost fluid method Fedkiw *et al.* (1999). An algorithm that reconstructs the liquid velocity in the gas and the gas velocity in the liquid is then employed, ensuring that the velocity field is continuous while allowing for discontinuous gradients at the interface. These two methods are evaluated on a droplet convection test case, and both are found to improve significantly the robustness of the simulations.

1. Introduction

Turbulent liquid-gas flows are found in many natural phenomena and engineering devices. Consequently, the numerical simulation of such flows has been the focus of a significant body of work. Several key challenges are classically associated with such simulations. In particular, the discontinuity in the material properties of the fluids, in particular density and viscosity, as well as the existence of a singular surface tension force, complicate the discretization of the governing equations at the interface.

Two main methods have been employed to handle the discontinuities in the flow field. First, the continuum surface force (CSF) approach proposed by Brackbill *et al.* (1992) smears out the discontinuities in density and viscosity until they can be resolved by the computational mesh. Similarly, the surface tension force is added to the Navier-Stokes equation in the form of a body force. On the other hand, the ghost fluid method (GFM) (Fedkiw *et al.* 1999) treats the singularities of two-phase flows explicitly using generalized Taylor series expansions that account for jumps. Because it is true to the discontinuous nature of two-phase flows, the GFM is employed in this work.

Regardless of the methodology employed, incompressible two-phase flow simulations become more and more challenging to perform as the density ratio increases (Gorokhovski & Herrmann 2008). This is explained in part by looking at the pressure Poisson equation often used to enforce the solenoidal nature of the velocity field. This equation, written

$$\nabla \cdot \frac{1}{\rho} \nabla p = \frac{1}{\Delta t} \nabla \cdot \boldsymbol{u}, \tag{1.1}$$

becomes ill-conditioned because of the discontinuous nature of the coefficients of the

† Mechanical Engineering, University of Colorado at Boulder, Boulder, CO, USA
‡ CORIA, CNRS UMR6614, Université et INSA de Rouen, Saint-Etienne du Rouvray, France

modified Laplacian operator on the left-hand side of the equation. However, several methods have been proposed to solve this equation efficiently despite discontinuities in the Laplacian operator (MacLachlan *et al.* 2008). In this work, both the black-box multigrid (BBMG) solver of Dendy (1982) and the deflated conjugate gradient method (Saad *et al.* 2000) are employed. Both methods show excellent convergence properties regardless of the density ratio, confirming their capability of handling discontinuous operators.

Transport inconsistencies between density and velocity give rise to additional difficulties, as spurious errors in momentum can appear, leading to spurious variations in kinetic energy. This problem is exacerbated by the presence of strong shear at the interface and high density ratios, and ultimately causes numerical stability issues. Note that it can affect both level set (Sethian 1999) and volume of fluid methods (VOF) (Scardovelli & Zaleski 1999), since these approaches rely on very specific strategies for transporting the phase-interface, which are likely to differ from the way momentum is convected. In the context of VOF, Rudman (1998) suggested using VOF density fluxes when calculating the momentum convection term, thereby forcing a discrete compatibility between density and momentum transport. This first strategy for dealing with high density ratio flows was then adapted to level set methods by Raessi (2008) and Raessi & Pitsch (2009), although their work was limited to one- and two-dimensional problems.

Another potential solution to the non-physical kinetic energy variations at the phase interface is to use a two-velocity GFM. The concept behind a two-velocity GFM is to introduce two distinct velocity fields, one for the gas and one for the liquid, such that both liquid and gas velocities are defined in the entire domain, regardless of the phase. Then, interfacial boundary conditions can be used to reconnect the two velocity fields. This strategy has been simultaneously introduced by Tanguy *et al.* (2007) and Gibou *et al.* (2007) in order to simulate two-phase flows with heat and mass transfer, but it was not intended nor was it tested for high shear and high density ratio flows. Since the two-velocity GFM is capable of handling the discontinuous velocity fields that arise when considering evaporation, it is reasonable to postulate it will be capable of better handling high interfacial shear. In addition, since it uses the interface location to couple the liquid and the gas velocities, it can be expected to improve the consistency between interface and momentum transport.

In this paper, we investigate the capability of both strategies to improve the robustness and accuracy of high density ratio two-phase flow simulations. We make use of the accurate conservative level set (ACLS) method (Desjardins *et al.* 2008*b*) in both the NGA code (Desjardins *et al.* 2008*a*) and the YALES2 code. First, the density-based flux correction scheme proposed by Rudman (1998) for VOF schemes is adapted to level set methods. We introduce a different approach from that of Raessi (2008) and Raessi & Pitsch (2009), that can be easily formulated in three dimensions. While it is limited to first-order accuracy in this work, extension to second-order accurate schemes is possible. Then, a two-velocity GFM is presented. A new pressure jump is derived in order to couple the two velocities, and an algorithm that extends the liquid velocity in the gas and the gas velocity in the liquid is employed. Both approaches are shown to be viable options for handling high density ratio problems.

This paper is organized as follows. The mathematical formulation used in this work is presented in Section 2, along with a brief description of the ACLS method. Section 3 presents the density-based flux correction scheme, while Section 4 describes the two-velocity GFM. Finally, conclusions are drawn in Section 5.

2. Mathematical formulation

2.1. *Fluid equations*

Many gas-liquid flows can be described using the continuity and Navier-Stokes equations. Assuming both phases are incompressible, i.e., $\nabla \cdot \boldsymbol{u} = 0$, the continuity equation is written

$$\frac{D\rho}{Dt} = \frac{\partial \rho}{\partial t} + \boldsymbol{u} \cdot \nabla \rho = 0, \tag{2.1}$$

where $\boldsymbol{u}$ is the velocity field and ρ is the density. The Navier-Stokes equations are written

$$\frac{\partial \rho \boldsymbol{u}}{\partial t} + \nabla \cdot (\rho \boldsymbol{u} \otimes \boldsymbol{u}) = -\nabla p + \nabla \cdot \left(\mu \left[\nabla \boldsymbol{u} + \nabla \boldsymbol{u}^{\mathsf{T}}\right]\right) + \rho \boldsymbol{g}, \tag{2.2}$$

where p is the pressure, $\boldsymbol{g}$ is the gravitational acceleration, and μ is the dynamic viscosity.

The material properties are considered to be constant in each phase. The subscript l is used to describe the density and the viscosity in the liquid, respectively ρ_l and μ_l. Similarly, the subscript g corresponds to the density and the viscosity in the gas, respectively ρ_g and μ_g. It is convenient to introduce the jump of these quantities across the phase-interface Γ, defined by $[\rho]_\Gamma = \rho_l - \rho_g$ and $[\mu]_\Gamma = \mu_l - \mu_g$. In the absence of mass transfer between the two phases, the velocity field is continuous across Γ, i.e., $[\boldsymbol{u}]_\Gamma = 0$. In contrast, the existence of surface tension forces will lead to a discontinuity in the normal stresses at the gas-liquid interface. This translates into a pressure jump that can be expressed as

$$[p]_\Gamma = \sigma \kappa + 2 [\mu]_\Gamma \boldsymbol{n}^{\mathsf{T}} \cdot \nabla \boldsymbol{u} \cdot \boldsymbol{n}, \tag{2.3}$$

where σ is the surface tension coefficient, κ is the curvature of the phase-interface, and $\boldsymbol{n}$ is the phase-interface normal.

2.2. *Accurate conservative level set approach*

According to the level set methodology, the interface is defined implicitly as an iso-surface of a smooth function ψ, and is transported by solving

$$\frac{\partial \psi}{\partial t} + \nabla \cdot (\boldsymbol{u} \psi) = 0. \tag{2.4}$$

Note that since the velocity field is solenoidal, this equation implies that the phase-interface undergoes material transport, in accordance with Eq. 2.1. In ACLS (Desjardins *et al.* 2008*b*), the level set function is defined as an hyperbolic tangent profile, written

$$\psi(\boldsymbol{x}, t) = \frac{1}{2}\left(\tanh\left(\frac{\phi(\boldsymbol{x}, t)}{2\epsilon}\right) + 1\right), \tag{2.5}$$

where ϵ is a parameter that sets the thickness of the profile. We set ϵ to half the characteristic cell size in all simulations in this paper. In the previous equation, ϕ corresponds to a standard signed distance function, i.e.,

$$|\phi(\boldsymbol{x}, t)| = |\boldsymbol{x} - \boldsymbol{x}_\Gamma|, \tag{2.6}$$

where $\boldsymbol{x}_\Gamma$ corresponds to the closest point on the interface from $\boldsymbol{x}$, and $\phi(\boldsymbol{x}, t) > 0$ on one side of the interface, and $\phi(\boldsymbol{x}, t) < 0$ on the other side. Finally, a reinitialization equation is introduced in order to preserve the hyperbolic tangent profile. This equation is written

$$\frac{\partial \psi}{\partial \tau} + \nabla \cdot (\psi(1 - \psi)\boldsymbol{n}) = \nabla \cdot (\epsilon(\nabla \psi \cdot \boldsymbol{n})\boldsymbol{n}), \tag{2.7}$$

and is solved in pseudo-time τ at each time-step. This approach is chosen because it combines the accuracy of level set methods with excellent conservation properties. The ACLS methodology, in particular its coupling with the GFM, is described in more details by Desjardins *et al.* (2008).

3. A density-based flux correction scheme

In order to improve the robustness of high density ratio two-phase flow simulations, we first investigate the approach proposed by Rudman (1998). This approach consists of building density fluxes from the interface transport scheme, and then using those fluxes when constructing momentum convection fluxes. Rudman's approach was first introduced in the context of VOF schemes, where density fluxes are readily available from volume fraction advection. Raessi (2008) and Raessi and Pitsch (2009) then extended this idea to level set methods, using geometric arguments to construct density fluxes from the level set field at the old and new time-step, t^n and t^{n+1}.

3.1. *Methodology*

The Navier-Stokes equations are advanced by solving

$$\frac{\boldsymbol{u}^{\star}_{k+1} - \boldsymbol{u}^n}{\Delta t} = P_k^{n+\frac{1}{2}} - C_{k+1}^{n+\frac{1}{2}} - V_{k+1}^{n+\frac{1}{2}}, \tag{3.1}$$

where

$$P_k^{n+\frac{1}{2}} = -\frac{1}{\rho^{n+\frac{1}{2}}} \nabla p_k^{n+\frac{1}{2}}, \tag{3.2}$$

$$C_{k+1}^{n+\frac{1}{2}} = \nabla \cdot \left(\boldsymbol{u}_{k+1}^{n+\frac{1}{2}} \otimes \boldsymbol{u}_{k+1}^{n+\frac{1}{2}} \right), \tag{3.3}$$

$$\text{and} \quad V_{k+1}^{n+\frac{1}{2}} = \frac{1}{\rho^{n+\frac{1}{2}}} \nabla \cdot \left(\mu^{n+\frac{1}{2}} \left[\nabla \boldsymbol{u}_{k+1}^{n+\frac{1}{2}} + \nabla \boldsymbol{u}_{k+1}^{n+\frac{1}{2}} \Big|^{\mathsf{T}} \right] \right) \tag{3.4}$$

are the pressure, convective, and viscous terms, respectively. The spatial discretization of these three terms is discussed in detail in Desjardins *et al.* (2008*a*), and the specific adjustments to the discretization due to the multiphase nature of the flow are discussed in Desjardins *et al.* (2008*b*) and Desjardins and Pitsch (2009) for both the pressure term and the viscous term. In these equations, the index k represents the iteration number. At $k = 0$, we use $\boldsymbol{u}_0^{n+1} = \boldsymbol{u}^n$, and $p_0^{n+\frac{1}{2}} = p^{n-\frac{1}{2}}$. In addition, note that the convective and viscous terms are expressed using $k+1$, making Eq. 3.1 implicit. This is handled using an approximate factorization technique similar to that of Choi and Moin (1994). The intermediate velocity field $\boldsymbol{u}^{\star}_{k+1}$ is then made solenoidal by solving the pressure Poisson equation,

$$\nabla \cdot \left(\frac{1}{\rho^{n+\frac{1}{2}}} \nabla p_{k+1}^{n+\frac{1}{2}} \right) = \frac{1}{\Delta t} \nabla \cdot \boldsymbol{u}^{\star}_{k+1}, \tag{3.5}$$

and then applying

$$\boldsymbol{u}_{k+1}^{n+1} = \boldsymbol{u}^{\star}_{k+1} - \frac{\Delta t}{\rho^{n+\frac{1}{2}}} \nabla p_{k+1}^{n+\frac{1}{2}}. \tag{3.6}$$

3.2. *Density-based momentum flux correction*

In order to improve the coupling between momentum convection and level set transport, $C_{k+1}^{n+\frac{1}{2}}$ is modified to include a density $\widehat{\rho}$, which will be constructed from the level set. The

new convection term $\widehat{C}_{k+1}^{n+\frac{1}{2}}$ is obtained by recasting Eq. 3.1 in terms of the momentum instead of the velocity, giving (ignoring pressure and viscosity for convenience)

$$\frac{\hat{\rho}^{n+1}\boldsymbol{u}_{k+1}^{\star} - \hat{\rho}^{n}\boldsymbol{u}^{n}}{\Delta t} = -\nabla\cdot\left(\hat{\rho}^{n+\frac{1}{2}}\boldsymbol{u}_{k+1}^{n+\frac{1}{2}}\otimes\boldsymbol{u}_{k+1}^{n+\frac{1}{2}}\right), \tag{3.7}$$

from which the new form of the convection term is found to be

$$\widehat{C}_{k+1}^{n+\frac{1}{2}} = \frac{1}{\hat{\rho}^{n+1}}\nabla\cdot\left(\hat{\rho}^{n+\frac{1}{2}}\boldsymbol{u}_{k+1}^{n+\frac{1}{2}}\otimes\boldsymbol{u}_{k+1}^{n+\frac{1}{2}}\right) + \frac{1}{\hat{\rho}^{n+1}}\frac{\hat{\rho}^{n+1}\boldsymbol{u}^{n} - \hat{\rho}^{n}\boldsymbol{u}^{n}}{\Delta t}. \tag{3.8}$$

Equation 3.1 is then replaced by

$$\frac{\boldsymbol{u}_{k+1}^{\star} - \boldsymbol{u}^{n}}{\Delta t} = P_{k}^{n+\frac{1}{2}} - \widehat{C}_{k+1}^{n+\frac{1}{2}} - V_{k+1}^{n+\frac{1}{2}}. \tag{3.9}$$

Since the new convective term involves density, which can vary by orders of magnitude from one cell to another, great care is needed when defining $\hat{\rho}$.

3.3. *Definition of the density*

The density that appears in the new convective term can be defined in multiple ways from the level set field ψ (which can be replaced by ϕ without loss of generality), i.e., $\hat{\rho} = \hat{\rho}(\psi)$. For example, we could calculate the liquid volume fraction in each cell using the second-order accurate algorithm of van der Pijl (2005). Note that $\hat{\rho}^{n+\frac{1}{2}}$ only needs to be defined at the location of the velocity flux $\widehat{C}_{k+1}^{n+\frac{1}{2}}$, while $\hat{\rho}^{n}$ and $\hat{\rho}^{n+1}$ need to be known at the same location as the velocity components. Because we make use of a staggered variable arrangement where the level set is defined at the cell center (corresponding to cell indices $i-\frac{1}{2}$, $i+\frac{1}{2}$, etc.) and the velocity components are defined at the cell faces (corresponding to i, $i+1$, etc.), we start by writing

$$\hat{\rho}_{i}^{n} = \rho_{g} + [\rho]_{\Gamma}\, h\left(\phi_{i-\frac{1}{2}}^{n}, \phi_{i+\frac{1}{2}}^{n}\right), \tag{3.10}$$

where the height function h is defined by

$$h\left(\phi_{i-\frac{1}{2}}^{n}, \phi_{i+\frac{1}{2}}^{n}\right) = \begin{cases} 1 & \text{if } \phi_{i-\frac{1}{2}}^{n} \geq 0 \text{ and } \phi_{i+\frac{1}{2}}^{n} \geq 0 \\ 0 & \text{if } \phi_{i-\frac{1}{2}}^{n} < 0 \text{ and } \phi_{i+\frac{1}{2}}^{n} < 0 \\ \frac{\phi_{i-\frac{1}{2}}^{n+} + \phi_{i+\frac{1}{2}}^{n+}}{|\phi_{i-\frac{1}{2}}^{n}| + |\phi_{i+\frac{1}{2}}^{n}|} & \text{otherwise,} \end{cases} \tag{3.11}$$

where $a^{+} = \max(a, 0)$. Next, $\hat{\rho}^{n+\frac{1}{2}}\boldsymbol{u}_{k+1}^{n+\frac{1}{2}}$ is treated as a density flux for the continuity equation, allowing us to write

$$\hat{\rho}^{n+1} = \hat{\rho}^{n} - \Delta t\nabla\cdot\left(\hat{\rho}^{n+\frac{1}{2}}\boldsymbol{u}_{k+1}^{n+\frac{1}{2}}\right). \tag{3.12}$$

Since Rudman (1998) was working with VOF, these density fluxes were readily available. With a level set scheme, these need to be reconstructed from the level set field. Raessi (2008) proposed using the old and new level set fields, ϕ^{n} and ϕ^{n+1}, for that purpose. While simple and elegant in one dimension, this approach poses a bigger challenge in two and three dimensions. Indeed, creating a density flux from a temporal variation in the level set field requires inverting a divergence operator, which is simple to do in one dimension, but non-unique in two or more dimensions.

Instead, we propose using both the level set and the velocity data at time t^{n} in order

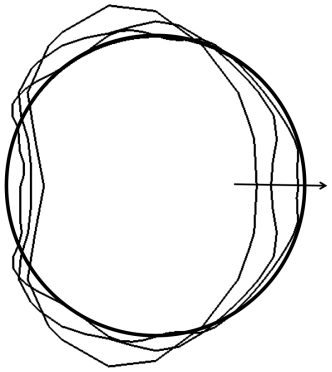

FIGURE 1. Droplet shape after one flow-through time using the density-based momentum flux correction scheme. The arrow indicates mesh size increasing from 32^2 to 64^2 to 128^2, and the thick line is the exact solution.

to form a useable flux. Note that boundedness is a critical requirement when defining this flux, since we want to make use of Eq. 3.12 to define $\hat{\rho}^{n+1}$. Hence, a simple upwinded scheme is a good candidate, and we write

$$\hat{\rho}^{n+\frac{1}{2}}_{i+\frac{1}{2}} = \begin{cases} \hat{\rho}^n_i & \text{if } \boldsymbol{u}^{n+\frac{1}{2}}_{k+1}\Big|_{i+\frac{1}{2}} \geq 0 \\ \hat{\rho}^n_{i+1} & \text{otherwise.} \end{cases} \tag{3.13}$$

Equations 3.10, 3.13, and 3.12 define all the density terms that appear in Eq. 3.8, thereby completing the definition of the corrected convective flux. This approach ensures a tight coupling between level set and momentum transport, since $\hat{\rho}^n$ is defined directly from the level set at each time-step. While this scheme is first-order in both space and time, more accurate schemes can readily be used provided they maintain the boundedness of $\hat{\rho}^{n+1}$. Finally, note that the extension to three dimensions is straightforward.

3.4. *Convection of a high density droplet*

This momentum correction scheme is evaluated on a simple two-dimensional test case of droplet transport. A droplet of diameter D is placed in the middle of a periodic computational domain of size $5D \times 5D$. Various meshes are considered, ranging from 32^2 to 128^2. The velocity field is initialized by giving the liquid a velocity $u_l = 1$ and $v_l = 0$, while the gas is initially at rest. The time-step size is chosen such that the convective CFL remains below 0.2. Both gas and liquid viscosities, as well as the surface tension coefficient, are set to zero. Finally, the density ratio between the liquid and the gas is set to 10^6. Under these conditions, the droplet is expected to remain perfectly circular. However, the non-corrected scheme described in Section 3.1 becomes unstable and fails in less than a third of a flow-through time regardless of the mesh refinement or time-step size. In comparison, the density-corrected scheme runs robustly with all meshes for any number of flow-through times. Some deformation of the drop is visible, although it does not appear to increase significantly with time. Figure 1 shows the phase-interface after one flow-through time for the various meshes, compared to the exact solution. The drop shape converges satisfyingly toward the exact solution.

4. A first-order two-velocity ghost fluid method

4.1. *Derivation of the method*

The GFM relies on the extension of the pressure jump conditions away from the interface located at $\boldsymbol{x}_\Gamma$ through a Taylor series expansion

$$[p](\boldsymbol{x}) = [p]_\Gamma + (\boldsymbol{x} - \boldsymbol{x}_\Gamma) \cdot [\nabla p]_\Gamma + \mathcal{O}\left((\boldsymbol{x} - \boldsymbol{x}_\Gamma)^2\right) . \tag{4.1}$$

In order to obtain a first-order GFM, both the pressure jump $[p]_\Gamma$ and the pressure gradient jump $[\nabla p]_\Gamma$ at the interface have to be prescribed. The pressure jump $[p]_\Gamma$ may be expressed as a function of surface tension and viscous forces at the interface, as seen in Eq. 2.3. However, the pressure gradient jump has to be prescribed from the known variables in both phases. In the single-velocity first-order GFM, this jump comes from the hypothesis that the density-weighted pressure gradient $\nabla p/\rho$ is continuous at the interface. This assumption is no longer applicable when transporting two velocities because the velocity predictors in both phases $\boldsymbol{u}_l^\star$ and $\boldsymbol{u}_g^\star$ may be discontinuous at the interface, which leads to a jump in the density-weighted pressure gradient. To generalize the first-order GFM to discontinuous predictors, one can assume that the pressure correction step is valid at the interface in both phases, i.e.,

$$\frac{\boldsymbol{u}_l^{n+1} - \boldsymbol{u}_l^\star}{\Delta t} = -\frac{1}{\rho_l} \nabla p_l \,, \quad \frac{\boldsymbol{u}_g^{n+1} - \boldsymbol{u}_g^\star}{\Delta t} = -\frac{1}{\rho_g} \nabla p_g \,. \tag{4.2}$$

Then, taking the difference of the two previous equations, one obtains the following relation between jump conditions,

$$\frac{\left[\boldsymbol{u}^{n+1}\right]_\Gamma - \left[\boldsymbol{u}^\star\right]_\Gamma}{\Delta t} = -\left[\frac{1}{\rho} \nabla p\right]_\Gamma . \tag{4.3}$$

If the jump condition for the velocity at time t^{n+1} is prescribed, the pressure gradient jump may be expressed from the density-weighted pressure gradients as

$$[\nabla p]_\Gamma = \rho_l \left[\frac{1}{\rho} \nabla p\right]_\Gamma + [\rho]_\Gamma \frac{1}{\rho_g} \nabla p_g = \rho_l \frac{\left[\boldsymbol{u}^\star\right]_\Gamma - \left[\boldsymbol{u}^{n+1}\right]_\Gamma}{\Delta t} + [\rho]_\Gamma \frac{1}{\rho_g} \nabla p_g \,, \tag{4.4}$$

$$= \rho_g \left[\frac{1}{\rho} \nabla p\right]_\Gamma + [\rho]_\Gamma \frac{1}{\rho_l} \nabla p_l = \rho_g \frac{\left[\boldsymbol{u}^\star\right]_\Gamma - \left[\boldsymbol{u}^{n+1}\right]_\Gamma}{\Delta t} + [\rho]_\Gamma \frac{1}{\rho_l} \nabla p_l \,. \tag{4.5}$$

These expressions may then be used to compute the pressure gradient. For instance, given a 1D problem with the centroid of control volume i in the gas and the centroid of control volume $i+1$ in the liquid, separated by a distance Δx, $\theta = (x_\Gamma - x_i)/\Delta x$, and $\rho' = \theta\rho_g + (1-\theta)\rho_l$, the second-order pressure gradient in the gas reads

$$\frac{1}{\rho_g} \frac{p_{g,i+1} - p_{g,i}}{\Delta x} = \frac{1}{\rho_g} \frac{p_{l,i+1} - [p]_{i+1} - p_{g,i}}{\Delta x} \,, \tag{4.6}$$

and using Eq. 4.1,

$$\frac{1}{\rho_g} \frac{p_{g,i+1} - p_{g,i}}{\Delta x} = \frac{1}{\rho_g} \frac{p_{l,i+1} - p_{g,i}}{\Delta x} - \frac{1}{\rho_g} \frac{[p]_\Gamma}{\Delta x} - \frac{1}{\rho_g} (1-\theta) \left[\nabla p\right]_\Gamma . \tag{4.7}$$

The pressure gradient jump $[\nabla p]_\Gamma$ may be replaced by its expression in Eq. 4.4 and after some rearrangements, the pressure gradient in the gas is

$$\frac{1}{\rho_g} \frac{p_{g,i+1} - p_{g,i}}{\Delta x} = \frac{1}{\rho'} \frac{p_{l,i+1} - p_{g,i}}{\Delta x} - \frac{1}{\rho'} \frac{[p]_\Gamma}{\Delta x} - \frac{\rho_l}{\rho'} (1-\theta) \frac{\left[\boldsymbol{u}^\star\right]_\Gamma - \left[\boldsymbol{u}^{n+1}\right]_\Gamma}{\Delta t} \,. \tag{4.8}$$

The same type of expression may be obtained for the pressure gradient in the liquid,

$$\frac{1}{\rho_l}\frac{p_{l,i+1}-p_{l,i}}{\Delta x}=\frac{1}{\rho'}\frac{p_{l,i+1}-p_{g,i}}{\Delta x}-\frac{1}{\rho'}\frac{[p]_\Gamma}{\Delta x}+\frac{\rho_g}{\rho'}\theta\frac{[\boldsymbol{u}^\star]_\Gamma-\left[\boldsymbol{u}^{n+1}\right]_\Gamma}{\Delta t}\,. \tag{4.9}$$

To make the link with the single-velocity GFM, note that Eqs. 4.8 and 4.9, combined with Eq. 4.2, both lead to

$$\frac{1}{\rho'}\frac{p_{l,i+1}-p_{g,i}}{\Delta x}=\frac{1}{\rho'}\frac{[p]_\Gamma}{\Delta x}+\frac{1}{\rho'}\frac{(\rho\boldsymbol{u}^\star)'-(\rho\boldsymbol{u}^{n+1})'}{\Delta t}\,. \tag{4.10}$$

This expression is very similar to the one obtained for the single-velocity GFM, except for the second term of the RHS where a density weighting appears. Finally, the Poisson equation to compute the pressure is found by taking the divergence of Eq. 4.10 at the interface and Eq. 4.2 away from the interface. Note that the resolution of the Poisson equation will only give the values of p_l in the liquid and p_g in the gas. Hence, the liquid and gas pressure gradients will be known only in their respective phase and across the interface. This implies that the liquid velocity cannot be updated from this pressure gradient in the gas, and similarly that the gas velocity cannot be updated in the liquid. As a result, some sort of velocity extension algorithm is needed.

4.2. *Velocity extension*

The extension of the liquid and gas velocities to the other phase is of primary importance for numerical stability. Indeed, as the interface is transported, liquid control volumes may become gas control volumes, and vice versa. The conversion of ghost values into real values creates kinetic energy errors that can be limited if the velocity extension is done carefully. Several numerical tests were performed and it was observed that only monotonic extensions led to stable algorithms.

The algorithm for the velocity extension that was tested successfully is based on a marching method along the level set normal. Indeed, a simple equation may be solved to propagate outward a quantity defined at the interface (Aslam 2003)

$$\frac{d\boldsymbol{u}}{ds}=\boldsymbol{n}\cdot\nabla\boldsymbol{u}=0 \text{ with } \boldsymbol{u}=\boldsymbol{u}_\Gamma \text{ at } \boldsymbol{x}=\boldsymbol{x}_\Gamma\,, \tag{4.11}$$

where s is the curvilinear abscissa along the normals and $\boldsymbol{n}$ is the local unit normal oriented in the direction away from the interface. This equation has to be solved in a band around the level set, which may be achieved by a simple Jacobi algorithm and a first-order upwind scheme for the velocity gradient.

4.3. *Full algorithm*

From the two-velocity GFM and the monotonic velocity extension algorithm presented above, a two-phase flow solver may be designed. The main steps of the solver are the following:

(*a*) advance the interface,
(*b*) advance both velocities to get the velocity predictors $\boldsymbol{u}_l^\star$ and $\boldsymbol{u}_g^\star$,
(*c*) solve the Poisson equation,
(*d*) compute the pressure gradients in both phases from Eqs. 4.2 and 4.10,
(*e*) correct both velocities in their respective phase to obtain $\boldsymbol{u}_l^{n+1}$ and $\boldsymbol{u}_g^{n+1}$,
(*f*) and extend the liquid and gas velocities to the other phase using Eq. 4.11.

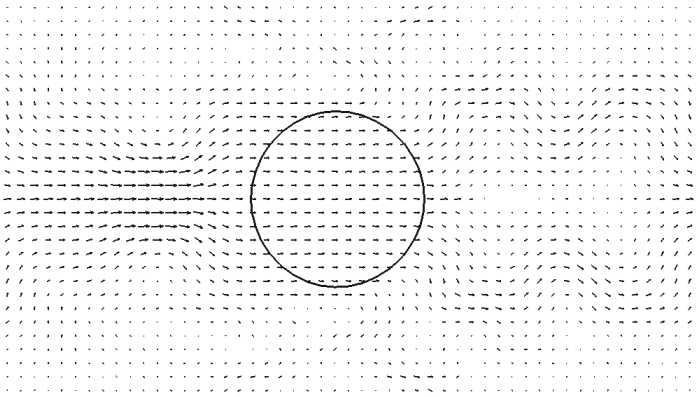

FIGURE 2. Velocity field and interface location after one flow-through time using the two-velocity GFM on a 64^2 mesh.

4.4. *Numerical example*

Finally, this approach is applied to the same droplet convection test case as that described in Section 3.4. The liquid velocity is initialized with a constant value $u_l = 1$, $v_l = 0$ in all the cells, while the gas is at rest in all the cells. Results obtained after one flow-through time on a 64^2 mesh are shown in Fig. 2. This figure shows the velocity field in the physical control volumes, as well as the location of the phase-interface. Even if the velocity is initialized as discontinuous at the interface, the algorithm imposes the given jump condition $\left[\boldsymbol{u}^{n+1}\right]_\Gamma = 0$ instantaneously through the pressure equation. As the Reynolds number is infinite and the density ratio is very large, many vortices develop in the gas whereas the velocity in the liquid remains essentially equal to its initial value. It may also be observed that the droplet maintains its initial form with excellent accuracy.

5. Conclusions

In this paper, two strategies for handling high density ratio two-phase flows are investigated. The first one is based on improving the consistency between level set and momentum transport through the introduction of a density in the momentum flux. This density has to be carefully defined from the level set at time t^n, then is updated to time t^{n+1} by solving the continuity equation. The density fluxes created in the process are then directly used to calculate the momentum fluxes in a discretely consistent manner. This strategy has the benefit of being both straightforward to implement and readily applicable to three-dimensional flows. It is shown to improve the robustness of two-phase flow simulations, allowing to us simulate a droplet with a density ratio of 10^6 in the absence of viscosity and surface tension while classical methods fail. The second strategy is based on a two-velocity GFM, where the gas and the liquid velocities are connected through a pressure jump condition. This approach is more involved since it requires two velocity fields to be carried in the algorithm, and since it involves an additional velocity extension scheme. However, it is shown to outperform the density-correction method, with the drop convection test case showing essentially no spurious drop deformation. In addition, such a scheme can readily be adapted to allow for mass transfer across the phase-interface. Further testing of both methods in the presence of strong shear and turbulence is warranted.

REFERENCES

Aslam, T. 2003 A partial differential equation approach to multidimensional extrapolation. *J. Comput. Phys.* **193**, 349–355.

Brackbill, J. U., Kothe, D. B. & Zemach, C. 1992 A continuum method for modeling surface tension. *J. Comput. Phys.* **100**, 335–354.

Choi, H. & Moin, P. 1994 Effects of the computational time step on numerical solutions of turbulent flow. *J. Comput. Phys.* **113**, 1–4.

Dendy, J. E. 1982 Black box multigrid. *J. Comput. Phys.* **48**, 366–386.

Desjardins, O., Blanquart, G., Balarac, G. & Pitsch, H. 2008*a* High order conservative finite difference scheme for variable density low Mach number turbulent flows. *J. Comput. Phys.* **227** (15), 7125–7159.

Desjardins, O., Moureau, V. & Pitsch, H. 2008*b* An accurate conservative level set/ghost fluid method for simulating primary atomization. *J. Comput. Phys.* **227** (18), 8395–8416.

Desjardins, O. & Pitsch, H. 2009 A spectrally refined interface approach for simulating multiphase flows. *J. Comput. Phys.* **228** (5), 1658–1677.

Fedkiw, R., Aslam, T., Merriman, B. & Osher, S. 1999 A non-oscillatory Eulerian approach to interfaces in multimaterial flows (the ghost fluid method). *J. Comput. Phys.* **152**, 457–492.

Gibou, F., Chen, L., Nguyen, D. & Banerjee, S. 2007 A level set based sharp interface method for the multiphase incompressible Navier–Stokes equations with phase change. *J. Comput. Phys.* **222** (2), 536–555.

Gorokhovski, M. & Herrmann, M. 2008 Modeling primary atomization. *Ann. Rev. Fluid Mech.* **40**, 343–366.

MacLachlan, S., Tang, J. & Vuik, C. 2008 Fast and robust solvers for pressure-correction in bubbly flow problems. *J. Comput. Phys.* **227**, 9742–9761.

van der Pijl, S. P., Segal, A. & Vuik, C. 2005 A mass-conserving level-set method for modelling of multi-phase flows. *Int. J. Numer. Meth. Fluids* **47**, 339–361.

Raessi, M. 2008 A level set based method for calculating flux densities in two-phase flows. In *Annual Research Briefs* (Center for Turbulence Research, Stanford).

Raessi, M. & Pitsch, H. 2009 Modeling interfacial flows with large density ratios. In *Annual Research Briefs* (Center for Turbulence Research, Stanford).

Rudman, M. 1998 A volume-tracking method for incompressible multifluid flows with large density variations. *International Journal for Numerical Methods in Fluids* **28**, 357–378.

Saad, Y., Yeung, M., Erhel, J. & Guyomarc'h, F. 2000 A deflated version of the conjugate gradient algorithm. *SIAM Journal on Scientific Computing* **21** (5), 1909–1926.

Scardovelli, R. & Zaleski, S. 1999 Direct numerical simulation of free-surface and interfacial flow. *Ann. Rev. Fluid Mech.* **31**, 567–603.

Sethian, J. A. 1999 *Level Set Methods and Fast Marching Methods*, 2nd edn. Cambridge, UK: Cambridge University Press.

Tanguy, S., Ménard, T. & Berlemont, A. 2007 A level set method for vaporizing two-phase flows. *J. Comput. Phys.* **221**, 837–853.